

**Research Article**

Investigation of the temperature effect on the mechanical properties of 3D printed composites

Hamed Tanabi ^a 

^aMechanical Engineering Department, University of Turkish Aeronautical Association, Ankara, Turkey

ARTICLE INFO

Article history:

Received 17 January 2021

Revised 20 February 2021

Accepted 01 March 2021

Keywords:

Additive manufacturing

FDM

Fiber reinforcement

Structural analysis

3D print

ABSTRACT

Short fiber reinforced additively manufactured components are lightweight yet durable materials with a wide range of potential applications in various industries such as aerospace and automotive. The fabricated specimens may be subjected to various thermal conditions ranging from -20 up to 60 °C during their service life. This study aims to investigate the effect of temperature on mechanical properties of the 3D printed short glass-fiber-reinforced polyamide 6 (GFPA6) composites and ABS as an unreinforced polymer. In accordance with ASTM D638, tensile test specimens were fabricated using Fused Deposition Modeling (FDM) technique. The fabricated samples were subjected to tensile load to investigate the stiffness and strength while temperatures set to -20, 20, 40, and 60 °C. The mechanisms of failure were identified based on fracture surface microscopic analysis. The glass fiber reinforced PA6 showed higher stiffness and strength up to 56% and 59% compare to ABS. At elevated temperatures, specimens showed a large deformation with a significant decline in tensile strength. It was observed that the dominant failure mechanism for ABS was the breakage of the deposited filaments while fiber pull-out was the dominant failure mechanism for GFPA6 material.

© 2021, Advanced Researches and Engineering Journal (IAREJ) and the Author(s).

1. Introduction

Additive manufacturing as a revolutionary technology has found so many applications in fabricating structural parts ranging from customized small to high performance parts. The benefits of this technology involve easy and fast prototyping of parts with complex shapes, low waste of raw materials, and affordable cost. Among the available additive manufacturing processes, Fused Deposition Modeling (FDM), is more interested respect to the low cost of the technology, minimal waste of material together with ease of access and use [1, 2]. In FDM, three-dimensional parts are fabricated using a layer-by-layer deposition of a thermoplastic polymer such as Poly Lactic Acid (PLA), nylon, Acrylonitrile butadiene styrene (ABS), and polycarbonate. Lack of toughness, strength, and unstable mechanical properties make the end-use FDM parts made from pure polymers, to be unreliable for structural and functional engineering applications [3]. However, this issue has been addressed by introducing fiber reinforced

filaments for FDM. In recent years, the study on printing process conditions and final properties of FDM parts reinforced with short or continuous carbon, glass, and aramid fibers is under extensive investigation [4–6].

In [7], continuous carbon fiber was used to reinforce FDM printed ABS, while PLA was used in [5, 8]. The mechanical characterization of the printed composites indicated that the bending and tensile strengths were increased respectively by up to 35% and 108% in comparison with pure PLA while delamination together with matrix cracking were found as the dominant failure modes [9].

Mohammadizadeh et al. [3] Studied the mechanical and structural behavior of the continuous carbon fiber reinforced 3D printed components under static and dynamic loadings. The presented results show that specimens printed with fiber inclusion exhibit superior mechanical properties compared with those fabricated with pure polymer. Also, fiber breakage, fiber pull-out,

* Corresponding author. Tel.: +90-312-589-6100.

E-mail addresses: htanabi@thk.edu.tr (H. Tanabi)

ORCID: 0000-0002-0911-6849 (H. Tanabi)

DOI: 10.35860/iarej.862304

This article is licensed under the CC BY-NC 4.0 International License (<https://creativecommons.org/licenses/by-nc/4.0/>).

and delamination were indicated as the dominant failure mechanisms.

The impact damage performance of FDM printed continuous glass, carbon, and aramid fiber reinforced thermoplastic composites was studied in [10]. The authors found that while the printed parts with carbon fiber reinforced nylon results in a brittle structure, the impact performance of the nylon reinforced with glass fibers was improved significantly.

Yasa and Ersoy [11] investigated the mechanical properties and dimensional accuracy of the short carbon fiber reinforced nylon composites fabricated by FDM. They showed that using appropriate compensation techniques the dimensional accuracy for some features can be enhanced. The presented results for tensile tests show that compared to unreinforced nylon, the elastic modulus and yield strength were greatly enhanced at the cost of ductility.

Yu et al. [12] used X-ray microscopy to characterize the internal morphologies of 3D-printed composites. They used Modified Kelly-Tyson model considering the void volume fraction to predict the tensile strength of 3D-printed composites. Fiber length, fiber orientation, and void content were determined using morphology characterization through X-ray microscopy.

The properties such as high dimensional stability, high level of strength, and stiffness at an affordable cost make fiber reinforced filaments an interesting material that opens new application fields in FDM printing [13, 14]. For instance, these high-performance 3D printing filaments are used in fabricating light-weight Unmanned Aerial Vehicle (UAV) structures as well as their payloads [15–17]. It is worth noting that aero-structures may be subjected to a wide range of temperatures during their service life. For example, a gimbal (the platform that is used for stabilizing the optic and thermal cameras on a UAV) should be able to show stable performance in a temperature ranging from $-20\text{ }^{\circ}\text{C}$ to $60\text{ }^{\circ}\text{C}$. Thus, the structures made using FDM method should also be able to meet the desired structural requirements in the mentioned temperature range. Although the working temperature is a critical challenge in the application of FDM based polymers in aerospace structures; there is no study in open source literature on this field.

This study aims to address this issue by investigating the mechanical properties of FDM specimens made of fiber reinforced polymer filament at various temperatures. The study starts with the explanation of the samples material and their manufacturing process in section 2. Then the tensile test procedure is explained in detail in section 3. In section 4, the experimental results are presented together with the discussion of these results. Finally, in section 5, key findings and conclusions obtained from this study are presented.

2. Material and sample preparation

2.1 Characterization of Filaments

Thermo-gravimetric analysis (TGA) was used to identify the glass fiber mass fraction in the GF30-PA6 filament. The variation of the filament weight was measured in the $15\text{ }^{\circ}\text{C}$ to $1000\text{ }^{\circ}\text{C}$ temperature interval with the temperature rate of $10\text{ }^{\circ}\text{C}/\text{min}$. TGA was conducted under a nitrogen atmosphere.

2.2 Fabrication of Samples

Test specimens were fabricated in accordance with ASTM D638-Type I, using the fused deposition modeling technique. As material, ABS and XSTRAND GF30-PA6 filament (1.75 mm diameter, developed by Owens) were used. XSTRAND GF30-PA6 is a polyamide base filament reinforced with short glass fibers. Properties such as good chemical and UV resistance and high wear resistance make polyamide reinforced filaments an interesting material for 3D printing purposes. The GF30-PA6 filaments are moisture sensitive so to ensure constant material properties the material was dried in an oven at $60\text{ }^{\circ}\text{C}$ for 48 hours.

The geometry of test specimens was generated using the SolidWorks software package. The model geometry was exported as a stereolithography file (STL) and loaded into a 3D printer slicing software package, namely “Z-Suite” then the process parameters were adjusted. Samples were fabricated by Zortrax M 200 printer. Due to the abrasive nature of fiber reinforced filaments, a hard steel nozzle diameter of 0.4 mm was used as the extruder. The printing speed is set to 40 mm/s with a layer height of 0.19 mm for all layers. Infill density, bed, and nozzle temperatures are set to 100% (solid), $80\text{ }^{\circ}\text{C}$, and $255\text{ }^{\circ}\text{C}$, respectively. For ABS material printing speed, bed and nozzle temperatures are set to 35 mm/s, $80\text{ }^{\circ}\text{C}$, and $275\text{ }^{\circ}\text{C}$, respectively. To improve 3D printer bed adhesion, a thin layer of glue stick was applied on the bed just before printing.

The arrangement of the models in slicing software and printed samples is shown in Figure 1. In total, 40 test coupons were fabricated for mechanical characterization.

2.3 Mechanical Characterization

Uniaxial tensile tests were performed on samples (fabricated as outlined in section 2.1) according to ASTM D638 under displacement control by straining at a rate of 1 mm/min using a universal tensile test machine (Tenson). Tensile tests were performed at -20 , 20 , 40 , and $60\text{ }^{\circ}\text{C}$. Test samples were kept in an oven or a freezer for 30 minutes in temperatures the same as their test temperatures. During the test, a heating pad with a control unit (Tk heat clamp, New Era) was used for heating the test samples up to 40 and $60\text{ }^{\circ}\text{C}$. On the other hand, a freeze spray (RS PRO Aerosol) was used to lower the temperature to around $-20\text{ }^{\circ}\text{C}$. To keep the temperature around the desired value ($-20\pm 5\text{ }^{\circ}\text{C}$), the

spraying was performed during the test, continuously.

To measure the temperature of the samples, a noncontact infra-red thermometer (AN200, Extech) was used. The experimental setup is shown in Figure 2.

3. Results and discussion

3.1 Thermo-gravimetric Analysis of the Filaments

TGA results are presented in Figure 3. According to the TGA results the reinforcement fiber content in the filament was determined to be 27%.

3.2 Mechanical Characterization

Table 1 presents the results of the tensile test for eight test configurations. The presented results are an average of 5 tests. At room temperature, the tensile strength of ABS samples was measured as 32 ± 2 MPa. The strains at tensile strength and breaking point are 3.6% and 4.8%, respectively. In [18], the elastic modulus, average tensile strength and corresponding strain for ABS were reported as 1.7 GPa, 29.5 MPa and 2.3%, respectively. In [19], tensile strength was measured as 34 MPa, and strain at break was reported as 8.6%. In [20] Young's modulus, tensile strength, and strain at failure were reported as 1.9 GPa, 32.8 MPa, and 9%. However, in both [19] and [20] a wide scattering was observed in the reported strain value (around $\pm 3\%$). It is worth noting that the obtained mechanical properties can diverge significantly depending on the supplier and their filament fabrication process [2].

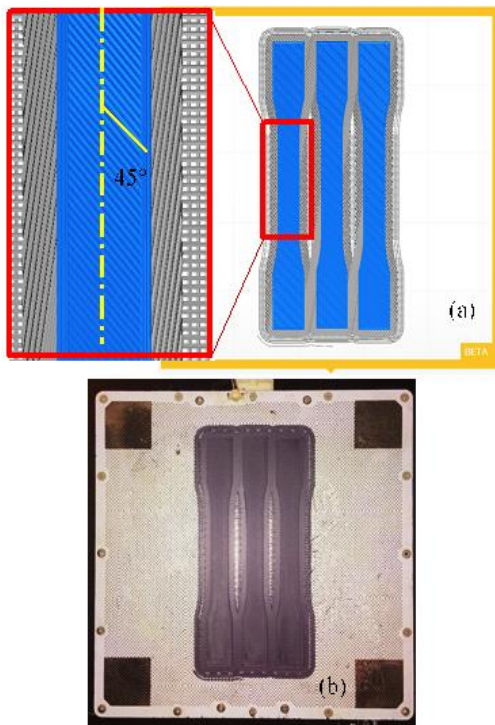


Figure 1. (a) Arrangement of the models in slicing software, Solid layers are oriented $\pm 45^\circ$, (b) Fabricated samples

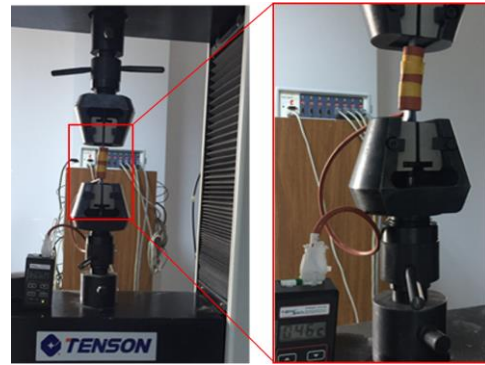


Figure 2. Tensile test and heating setups

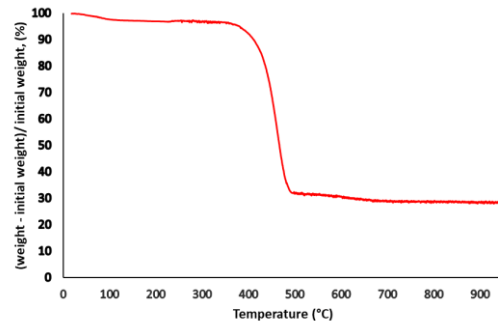


Figure 3. TGA analysis results of GFPA6 filaments

In all tests, elastic modulus decreases by increasing the temperature. For ABS material, the highest average modulus was measured at -20°C while by increasing temperature the elastic modulus was reduced significantly. Average tensile strength was also reduced by increasing the temperature, however, similar results were obtained at -20 and 20°C . For short glass fiber reinforced polyamide (GFPA6), a little variation in elastic modulus was observed for the tests performed at -20 and 20°C . However, average tensile strength is significantly affected by temperature and while a tensile strength of 70 ± 3 MPa was obtained at -20°C , it was measured as 51 ± 3 MPa, 30 ± 2 MPa, and 26 ± 2 MPa at 20 , 40 , and 60°C , respectively. For all test conditions, GFPA6 shows higher stiffness and tensile strength with respect to ABS.

For GFPA6, fracture strain is significantly increased by increasing the test temperature but is not affected at low (-20°C) temperature. For ABS, fracture strain does not vary too much in the temperature range of -20 to 40°C , but by increasing the temperature up to 60°C the fracture strain reaches 7.4%. Figure 4 shows stress versus strain diagrams of ABS and GFPA6 at various temperatures.

3.3 Characterization of the Fractured Surface

To determine the failure mechanism, all specimens were examined using an optical microscope. The images were obtained from the fracture surface of the samples. Optical microscopic images of the fractured surface of ABS and GFPA6 specimens are shown in Figure 4 and Figure 5, respectively.

Table 1. Uniaxial tensile test results for ABS and glass fiber reinforced PA6 at various temperatures

Sample	Material	Temperature (°C)	E (GPa)	S_{ut} (MPa)	ϵ (%)
ABS/-20C	ABS	-20±5	2.4±0.3	31±2	4.2±0.1
ABS/20C	ABS	20±2	1.6±0.3	32±2	4.8±0.2
ABS/40C	ABS	40±2	1.2±0.3	22±2	5.3±0.3
ABS/60C	ABS	60±2	1.1±0.2	15±3	7.4±0.5
GFPA6/-20C	GF30PA6	-20±5	3.0±0.3	70±3	5.0±0.1
GFPA6/20C	GF30PA6	20±2	2.5±0.2	51±3	5.2±0.1
GFPA6/40C	GF30PA6	40±2	1.5±0.2	30±2	9.8±0.3
GFPA6/60C	GF30PA6	60±2	1.3±0.2	26 ±2	8.4±0.3

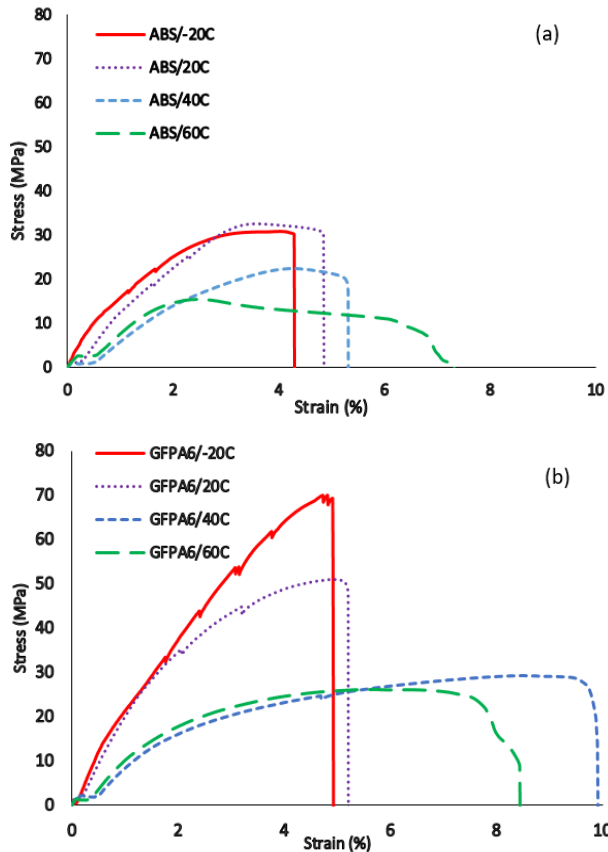


Figure 4. Stress vs strain diagram of a) ABS, and b) GFPA6

As it is shown in Figure 5, a local necking (narrowing in cross-section) is observed in ABS samples at 60 °C. The effect of this issue can also be traced on the stress vs. strain diagram of these samples (Figure 4a).

This phenomenon was not observed in GFPA6 samples. On the other hand, while a local fracture is seen in ABS/40C and ABS/60C specimens, fractured filaments are noticed in all over gauge length for ABS/-20C and ABS/20C (Figure 4). In all ABS test specimens, the fractured surface was perpendicular to the loading axis (Figure 5) while an oblique fracture surface was observed in GFPA6 samples (Figure 6).

The existence of voids and pores in 3D printed parts is unavoidable, though the shape, size, and distribution are highly dependent on the process parameters [21]. The internal structure and, in turn, the mechanical properties of the printed part are affected by these voids [22]. Internal voids result in a weak binding force between the deposited materials and serve as sites of cracks initiation and growth

through the fabricated structure by FDM process. The crack nucleation and propagation are manifested with fiber breakage, fiber pull-out, and delamination [3]. The fracture mechanism in ABS samples is fiber breakage while glass fiber pullout seems to be the main fracture mechanism in GFPA6 specimens. Chopped glass fibers in GFPA6, owing to higher elastic modulus, carry the highest load on the specimen. Thus, fiber pull-out is dominant

Takahashi et.al [23] showed that fiber pull-outs in loading direction is the main failure mechanism in short fiber reinforced polymers. Furthermore, they found that the number of pulled out fibers increases with increasing temperature. This phenomenon can be used to describe the variation in tensile strength of GFPA6 where at elevated temperatures the matrix-reinforcement fiber bonding strength is decreased thus, more fibers are pulled out even under low axial loads. In contrast, at low temperature (here is -20 °C) more axial load needs to overcome the matrix-reinforcement fiber bonding strength.

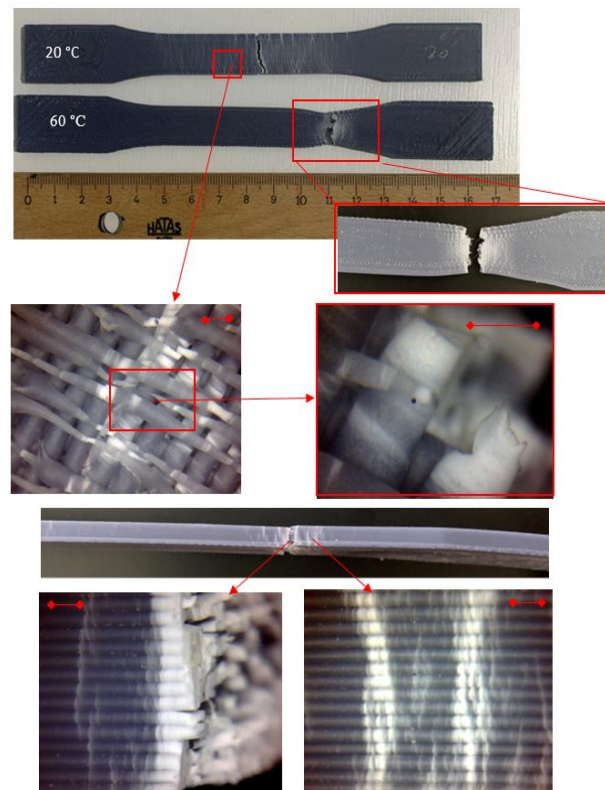


Figure 5. Optical images of ABS components after tensile test. Scale bar is 0.5 mm

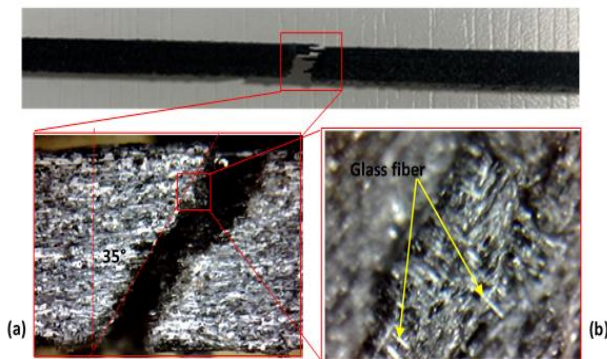


Figure 6. Optical images of GFPA6 component after the tensile test. The optic zoom is (a) 20X, (b) 400X

4. Conclusions

In this study, the effect of temperature on mechanical properties of 3D printed short glass fiber reinforced polyamide and ABS specimens under uniaxial tensile load were investigated experimentally. The fracture mode of the FDM printed composite samples was investigated using an optical microscope. Considering the experimental results the following conclusions were drawn from this work:

- Higher stiffness and strength up to 56% and 59% compare to ABS was obtained using glass fiber reinforced PA6.
- Both ABS and glass fiber reinforced PA6 specimens become stiffer at -20 C.
- At elevated temperatures, test specimens show a large deformation with a significant decline in tensile strength.
- For ABS, the breakage of the deposited filaments is the dominant failure mechanism.
- Reinforcement fiber pull-out was known as the dominant failure mechanism for GFPA6 material.

Declaration

The author declared no potential conflicts of interest with respect to the research, authorship, and/or publication of this article. The author also declared that this article is original, was prepared in accordance with international publication and research ethics, and ethical committee permission or any special permission is not required.

Author Contributions

H. Tanabi is responsible for all section of the study.

References

1. Dey A. and Yodo N. , *A systematic survey of FDM process parameter optimization and their influence on part characteristics*. Journal of Manufacturing and Materials Processing, 2019. 3(3).
2. Daminabo S.C., Goel S., Grammatikos S.A., Nezhad H.Y. and Thakur V.K., *Fused deposition modeling-based additive manufacturing (3D printing): techniques for polymer material systems*. Materials Today Chemistry, 2020. 16: p. 100248.
3. Mohammadzadeh M., Imeri A., Fidan I. and Elkelany M., *3D printed fiber reinforced polymer composites - Structural analysis*. Composites Part B, 2019. 175: p. 107112.
4. Mortazavian S. and Fatemi A., *Effects of fiber orientation and anisotropy on tensile strength and elastic modulus of short fiber reinforced polymer composites*. Composites Part B, 2015. 72: p. 116–129.
5. Tian X., Liu T., Yang C., Wang Q. and Li D., *Interface and performance of 3D printed continuous carbon fiber reinforced PLA composites*. Composites Part A: Applied Science and Manufacturing, 2016. 88: p. 198–205.
6. Justo J., Távora L. and París F., *Characterization of 3D printed long fibre reinforced composites*. Composite Structures, 2018. 185: p. 537–548.
7. Ning F., Cong W., Qiu J., Wei J. and Wang S., *Additive manufacturing of carbon fiber reinforced thermoplastic composites using fused deposition modeling*. Composites Part B: Engineering, 2015. 80: p. 369–378.
8. Li N., Li Y. and Liu S., *Rapid prototyping of continuous carbon fiber reinforced polylactic acid composites by 3D printing*. Journal of Materials Processing Technology, 2016. 238: p. 218–225.
9. Heidari-Rarani M., Rafiee-Afarani M. and Zahedi A.M., *Mechanical characterization of FDM 3D printing of continuous carbon fiber reinforced PLA composites*. Composites Part B: Engineering, 2019. 175: p. 107147.
10. Caminero M.A., Chacón J.M., García-moreno I. and Rodríguez G.P., *Impact damage resistance of 3D printed continuous fibre reinforced thermoplastic composites using fused deposition modelling*. Composites Part B, 2018. 148: p. 93–103.
11. Yasa E. and Ersoy K., *Dimensional Accuracy and Mechanical Properties of Chopped Carbon Reinforced Polymers Produced by Material Extrusion Additive Manufacturing*. Materials, 2019. 12(3885).
12. Yu S., Hyeong Y., Yeon J. and Hyung S., *Analytical study on the 3D-printed structure and mechanical properties of basalt fiber-reinforced PLA composites using X-ray microscopy*. Composites Science and Technology, 2019. 175: p. 18–27.
13. Attaran M., *The rise of 3-D printing: The advantages of additive manufacturing over traditional manufacturing*. Business Horizons, 2017. 60(5): p. 677–688.
14. Ngo T.D., Kashani A., Imbalzano G., Nguyen K.T.Q. and Hui D., *Additive manufacturing (3D printing): A review of materials, methods, applications and challenges*. Composites Part B: Engineering, 2018. 143: p. 172–196.
15. Azarov A. V, Antonov F.K., Golubev M. V, Khaziev A.R. and Ushanov S.A., *Composite 3D printing for the small size unmanned aerial vehicle structure*. Composites Part B, 2019. 169: p. 157–163.
16. Chen W. and Zhang Y., *Development and application of 3D printing technology in various fields*. Journal of Physics: Conference Series, 2019. 1303(1).
17. Moon S.K., Tan Y.E., Hwang J. and Yoon Y.J., *Application of 3D printing technology for designing light-weight unmanned aerial vehicle wing structures*. International Journal of Precision Engineering and Manufacturing - Green Technology, 2014. 1(3): p. 223–228.
18. Tymrak B.M., Kreiger M. and Pearce J.M., *Mechanical properties of components fabricated with open-source 3-D printers under realistic environmental conditions*. Materials and Design, 2014. 58: p. 242–246.

19. Torrado A.R., Shemelya C.M., English J.D., Lin Y., Wicker R.B. et al, *Characterizing the effect of additives to ABS on the mechanical property anisotropy of specimens fabricated by material extrusion 3D printing*. Additive Manufacturing, 2015. **6**: p. 16–29.
20. Cantrell J., Rohde S., Damiani D., Gurnani R., Disandro L. et al, *Experimental Characterization of the Mechanical Properties of 3D Printed ABS and Polycarbonate Parts*. 2017. **3**: p. 89–105.
21. Wang J., Xie H., Weng Z., Senthil T. and Wu L., *A novel approach to improve mechanical properties of parts fabricated by fused deposition modeling*. Materials and Design, 2016. **105**: p. 152–159.
22. Wang X., Zhao L., Ying J. and Fuh H., *Effect of Porosity on Mechanical Properties of 3D Printed Polymers: Experiments and Micromechanical Modeling Based on X-ray Computed Tomography Analysis*. Polymers (Basel), 2019. **11**(7): p. 1154.
23. Takahashi R., Shohji I., Seki Y. and Maruyama S., *Mechanical Properties of Short Fiber-Reinforced*. In: International Conference on Electronics Packaging (ICEP). JIEP, Toyama, pp 778–781.